Integrated Sensing and Communication in UAV Swarms for Cooperative Multiple Targets Tracking

Zhou, Longyu; Leng, Supeng; Wang, Qing; Liu, Qiang

DOI
10.1109/TMC.2022.3193499

Publication date
2023

Document Version
Final published version

Published in
IEEE Transactions on Mobile Computing

Citation (APA)
Zhou, L., Leng, S., Wang, Q., & Liu, Q. (2023). Integrated Sensing and Communication in UAV Swarms for Cooperative Multiple Targets Tracking. *IEEE Transactions on Mobile Computing*, *22*(11), 6526-6542. Article 9839387. https://doi.org/10.1109/TMC.2022.3193499

Integrated Sensing and Communication in UAV Swarms for Cooperative Multiple Targets Tracking

Longyu Zhou, *Graduate Student Member, IEEE*, Supeng Leng, *Member, IEEE*, Qing Wang, *Senior Member, IEEE*, and Qiang Liu, *Member, IEEE*

Abstract—Various interconnected Internet of Things (IoT) devices have emerged, led by the intelligence of the IoT, to realize exceptional interaction with the physical world. In this context, UAV swarm-enabled Multiple Targets Tracking (UAV-MTT), which can sense and track mobile targets for many applications such as hit-and-run, is an appealing topic. Unfortunately, UAVs cannot implement real-time MTT based on the traditional centralized pattern due to the complicated road network environment. It is also challenging to realize low-overhead UAV swarm cooperation in a distributed architecture for the real-time MTT. To address the problem, we propose a cyber-twin-based distributed tracking algorithm to update and optimize a trained digital model for real-time MTT. We then design a distributed cooperative tracking framework to promote MTT performance. In the design, both short-distance and long-distance distributed tracking cooperation manners are first realized with low energy consumption in communication by integrating resources of sensing and communication. Resource integration promotes target sensing efficiency with a highly successful tracking ratio as well. Theoretical derivation proves our algorithmic convergence. Hardware-in-the-loop simulation results demonstrate that our proposed algorithm can remarkably save 65.7% energy consumption in communication compared to other benchmarks while efficiently promoting 20.0% sensing performance.

Index Terms—Integrated sensing and communication, UAV swarm, target tracking, cyber-twin

1 Introduction

Unmanned Aerial Vehicle (UAV) as common aircraft can flexibly fly by autonomous control of an onboard computer. Owing to the advantages of versatility and low cost, UAVs can smoothly implement missions in numerous applications such as hit-and-run and emergency rescue [1], [2]. Against the backdrop of Artificial Intelligence (AI) technology, the popularity of UAV swarm-enable Multiple Targets Tracking (UAV-MTT) applications has triggered a surge to cooperatively search and track in a wealth of scenarios such as border patrol and space exploration. A swarm of UAVs not only can expand the network coverage area but also can lead to a data-gathering process [3], [4]. Take the hit-and-run as an instance, UAVs can discover those mobile targets affecting transportation security based on environmental observations. The observation can be transmitted to a center for tracking decisions, with which UAVs can automatically associate and track mobile targets.

For the traditional centralized pattern, the decision center is usually deployed on a base station [5]. In this context, UAVs cannot timely obtain tracking strategies due to remote physical transmission distance. A distributed pattern can shorten the transmission distance by exchanging information among neighbors [6], [7]. Nonetheless, this kind of exchange manner introduces new challenges to the MTT. First, for the large-scale UAV swarm, the exchange can be triggered when targets move out of the tracking range of current UAVs while not always ensuring tracking timeliness for those targets with high moving speeds. Then, the exchanged information may be highly redundant with overlapped sensing ranges that can incur a high energy consumption in communication. The overhead can negatively affect the real-time tracking performance. In addition, the information collected from the onboard sensors, such as the camera and lidar, is heterogeneous and massive which may lead to a high transmission latency. Finally, targets with flexible mobility can also pose severe pressure on the real-time requirement of MTT.

Fortunately, the Artificial Intelligence (AI) technology can provide great potential for real-time processing the heterogeneous data for low-latency communication and cooperative tracking performance [3]. The AI methodology enables agents to be self-trained for the optimal policy of UAV tracking cooperation. UAVs can real-time associate

- *Longyu Zhou and Supeng Leng are with the School of Information and Communication Engineering, University of Electric Science and Technology of China (UESTC), Chengdu 611731, China, and also with the Shenzhen Institute for Advanced Study, UESTC, Shenzhen 518000, China. E-mail: zhoulyfuture@outlook.com, spleng@uestc.edu.cn.*
- *Qing Wang is with the Department of Software Technology, Delft University of Technology, 2628, XE, Delft, The Netherlands. E-mail: qing.wang@tudelft.nl.*
- *Qiang Liu is with the School of Information and Communication Engineering, UESTC, Chengdu 611731, China, and also with the Yangtze Delta Region Institute, UESTC, Quzhou 324000, China. E-mail: liuqiang@uestc.edu.cn.*

Manuscript received 11 April 2022; revised 15 June 2022; accepted 20 July 2022. Date of publication 25 July 2022; date of current version 3 October 2023.
This work was supported in part by the National Key R&D Program of China under Grant 2018YFE0117500, and in part by the National Natural Science Foundation of China under Grant 61731006.
(Corresponding author: Supeng Leng.)
Digital Object Identifier no. 10.1109/TMC.2022.3193499

optimal mobile targets based on exchanged information with neighbors. The exchange manner can also assist UAVs in making and optimizing cooperative tracking decisions. However, it is intractable to reach a consensus on decisions with low-overhead communication performance in large-scale UAV swarm networks. Cyber-twin-based AI technology may be a feasible solution to meet the low-overhead communication requirement for real-time and cooperative MTT.

Based on the potential cyber-twin technology, each UAV can learn to obtain a customized digital model [8]. With the customized model, UAVs can share their learning information with neighbors for real-time tracking. The neighbors can transform their flight postures based on received information for highly efficient sensing. However, the learning complexity of the digital model may be significantly unacceptable once simulating multiple mobile targets simultaneously. In addition, frequent information exchange may be occurred to ensure informational effectiveness while causing tremendous challenges to limited communication resources and transmission reliability of the wireless MTT. With limited wireless bandwidth, ensuring the low-overhead UAV swarm cooperation becomes one of the bottlenecks for real-time MTT.

In this paper, we first design a distributed cooperative tracking framework. The framework realizes remote UAV cooperation based on Integrated Sensing and Communication (ISC). Afterward, we propose a cyber-twin-based distributed tracking algorithm to reduce tracking latency and improve target sensing abilities for the real-time MTT. Based on our algorithm, UAVs can adaptively transform beams of antennas with an interference-free characteristic to share learning information for exchanging reliability. The main contributions are summarized as follows.

- We first propose a cyber-twin-based distributed tracking algorithm in the UAV-MTT network. The algorithm can assist UAVs in learning a customized digital model to reduce energy consumption in communication. It can also acquire flight postures of neighbors to coordinate their tracking capabilities by rapid information exchange for real-time MTT. The model can be fast optimized and updated using our proposed algorithm with low synchronous convergence time. Furthermore, our algorithm can realize a lightweight mapping between the physical environment and the virtual world. The imitation complexity of mapping is significantly reduced by training partial observations based on our given attention mechanism.
- Based on the customized digital model, we design a new cooperative tracking framework. In this framework, each UAV can estimate the flight velocity of the target by the digital model. On the one hand, UAVs coordinate neighbors to implement proximal observation and tracking when their velocities match that of targets. On the other hand, based on historical tracking experiences, UAVs can also predict the trajectories of fast-moving targets to request the assistance of remote UAVs for subsequent tracking. Distal UAVs can rapidly fly to feasible airspace locations for standby tracking. It can significantly improve the successful tracking ratio. We can achieve both long- and short-distance cooperative tracking patterns to respond to diverse targets moving at different speeds in a distributed manner.
- To realize a low-overhead MTT, we integrate sensing and communication resources to promote mutual utilization. Unlike the traditional broadcasting manner, UAVs can rapidly align beams of antennas by sensing the spatial positions of receivers. It can ensure highly reliable information exchange with low-overhead communication. Furthermore, UAVs can use available sensing resources to select feasible relay UAVs quickly for efficient remote cooperation. The high-efficiency tracking performance is verified based on hardware-in-the-loop simulation compared to existing benchmarks.

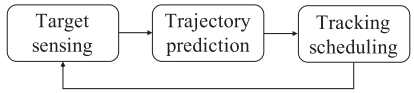

Fig. 1. General procedure in a Multiple Targets Tracking (MTT) system.

The rest of this paper is organized as follows. The background and related work are given in Section 2. Section 3 gives the system model. The optimization objective is formulated in Section 4. The ISC-based distributed tracking algorithm is designed in Section 5. The evaluation results are presented in Section 6. Finally, Section 7 concludes this paper and gives the future work.

2 Background and Related Work

2.1 Background

We first present some background information on the MTT and the cyber-twin system.

MTT: In an MTT system, multiple unknown targets can appear in an area of interest and move freely. These targets may cause potential dangers and their movements should be tracked. In this case, the trackers need to infer the targets' moving trajectories for monitoring and tracing [9], [10]. The flow diagram of a typical MTT system is given in Fig. 1. There are mainly three steps for tracking multiple targets in an MTT system: *target sensing, trajectory prediction, and tracking scheduling.* First, the trackers such as UAVs and cruisers should sense the mobile targets using onboard sensors (*target sensing*). Then, these sensors can collect more heterogeneous data such as the velocities and shapes of the targets. The data can be stored in caches of trackers or transmitted into the cloud to predict targets' trajectories (*trajectory prediction*). Finally, the results can conduct trackers to efficiently track targets for area security (*tracking scheduling*). The *advantage* of conventional MTT system is significant to support the arbitrary number of low-speed mobile targets based on the computing-intensive cloud. Meanwhile, the *weakness* is that *successful tracking ratio* reduces eventually when trackers track multiple high-speed mobile targets.

Cyber-twin: Cyber-twin is a virtual representation of the physical world. It not only can be a cyber mapping to reflect the status of physical entities but also can be a cyber thread to record the evolution of the physical world [11], [12]. Take

manufacturing as an example [13], cyber-twin can create a virtual model of a product such as an industrial robot. It can imitate the robot to enable virtual operations that provide valuable feedback by the cyber mapping interface for smooth task execution in the physical world. Furthermore, cyber-twin can analyze the recorded operation data to enhance manufacturing efficiency.

2.2 Related Work

In recent years, many researchers have exploited UAV networks for MTT. Many remarkable investigations are paid attention to the high-efficient MTT. Besides, some emerging applications such as cyber-twin technology are utilized for performance improvement.

Target Sensing: To cooperatively sense, the authors in [5] presented a vision-based target detection system that makes use of different capabilities of UAVs. The system can detect targets and find their positions in real-time. Considering the maritime scenario, the authors in [14] proposed a matched filter algorithm to exploit the Doppler dynamics of targets for accurate detection. To provide a robust target sensing, the authors in [15] proposed a new framework to combine adversarial learning with feature disentanglement modules for recognizing fine-grained targets such as gestures. However, these studies mainly utilize spectrum resources to facilitate cooperative sensing while the spectrum resource can be scarce in dense UAV swarm networks.

Trajectory Prediction and Interaction: Once targets are detected, UAVs can cooperatively predict trajectories of targets. The authors in [3] proposed a novel Deep Reinforcement Learning (DRL) approach to coordinate multiple UAVs to provide a highly accurate prediction solution. To reduce the position errors, the authors in [16] studied UAV swarm-based antenna arrays using beam-forming technology to exploit the position errors on the Angle-of-Arrival (AoA) estimation. To enhance interactive ability, the authors in [17] brought in an antenna array to boost the channel capability for backscatter communication cases. Nonetheless, existing researches mainly focus on cooperative computing based on the assumption of real-time and reliable data exchange in UAV swarm networks. A highly efficient communication scheme needs to be studied in some practical applications. The authors in [18] presented a comprehensive tutorial considering UAV benefits in a wide range of UAV applications. The communication problem is highlighted as an open challenge. To efficiently schedule communication resources in a UAV swarm, the authors in [19] considered an ultra-dense UAVs enabled content-centric wireless transmission network. The communication overhead is optimized based on a game method. The centralized pattern is not always feasible in many complicated MTT scenarios.

Tracking Scheduling: To optimize the tracking performance, the authors in [20] described a cooperative path planning algorithm to track a moving target in urban environments. It gave the optimal tracking paths for a moving target with low velocity. To ensure real-time tracking, the authors in [21] designed a novel tracking framework to accomplish simultaneous moving target tracking and path planning for minimal computing burden. Afterward, the authors in [22] proposed a Lyapunov-based mobile path following control law and a path-generation algorithm. The algorithm was estimated in practical scenarios for the optimization of energy consumption.

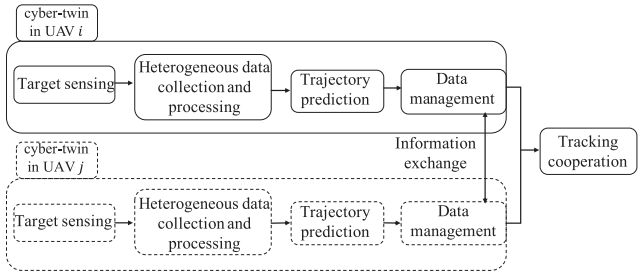

Fig. 2. Illustration of logic diagram in our UAV-MTT networks.

Cyber-Twin-Enabled MTT: Cyber-twin technology is applied to improve sensing coverage range and swarm tracking capability. The authors in [23] proposed a cover-set based target sensing algorithm. It could cluster targets to estimate their camera locations for large-scale coverage. Based on the designed $50\ m \times 50\ m$ tracking area, the algorithm realized over 60% sensing coverage for mobile targets with an average velocity of 28.8 km/h. However, the sensing performance may be reduced when tracking high-speed moving targets. For real-time tracking, the authors in [24] developed a model prediction method in a cyber-physical system. It could simultaneously realize trajectory planning and tracking control. It achieved that a single tracker avoided collision with other UAVs efficiently under 90 km/h high-speed mobile performance. The tracking performance with collision avoidance may be unacceptable when multiple trackers plan their tracking paths simultaneously. To achieve tracking cooperation, the authors in [25] proposed a novel dynamic fault-tolerant control model for cyber-physical systems. The model realized high tracking cooperation performance with an 80% fault-free ratio with 7 trackers. Cooperative tracking should be studied for algorithm scalability. In addition, the above studies mainly focus on tracking control while ignoring the communication overhead among trackers. The high complexity of the cover-set problem needs to be considered to ensure real-time MTT.

The aforementioned UAV-MTT researches mainly focus on tracking cooperation under the assumption of sufficient sensing and communication resources. Nonetheless, the communication requirement cannot always be satisfied in complicated MTT environments with limited accessible communication resources. An integrated sensing and communication method using the cyber-twin technology can be a potential solution to ensure communication quality while enhancing sensing performance for real-time UAV-MTT.

3 System Model

In this section, a cyber-twin-based cooperative tracking framework is designed to ensure UAV swarm cooperation in the UAV-MTT. To begin with, we give specific descriptions of the framework. Then, the information exchange model is formulated to qualify the communication-aware MTT.

The overall logical diagram is given in Fig. 2. We first discuss the target sensing based on onboard sensors in the

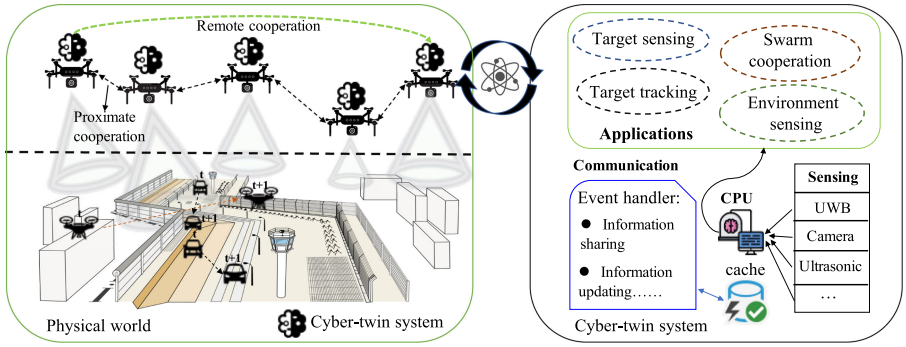

Fig. 3. Illustration of cooperative tracking framework.

physical world. The data is fed into the virtual world to implement heterogeneous data processing for high-efficient target estimation and trajectory prediction. Then, the processed data is stored in the cache of UAVs to support the information exchange with neighbors for accurate and real-time tracking cooperation.

We take hit-and-run as a typical instance shown in Fig. 3, UAVs can periodically take off to observe illegal vehicles. When K vehicles break traffic regulations to abscond, M UAVs can track the K illegal vehicles (targets) in the physical world. The UAV swarm is defined as a set $\mathcal{M} = \{1, 2, \ldots, M\}$ and the mobile targets are defined as a set $\mathcal{K} = \{1, 2, \ldots, K\}$. Each UAV can be an intelligent decision-maker with a virtual cyber-twin system [8], which can implement environmental sensing and modeling, sensing informational exchange, and self-driven learning. In the cyber-twin system, we constructively provide a swarm cooperative observation design to improve tracking performance. In the following elements, we will mainly discuss the cyber-twin system and beamforming based data transmission. The main symbols are also listed in Table 1.

Cyber-Twin Based Distributed Cooperation: The data is processed in the Manifold of UAVs for follow-up trajectory prediction and experiential learning for accurate target sensing and tracking. The cyber-twin models can acquire precise topology information, including positions, connectivity, and link qualities among neighbors. The information can assist UAVs in efficient information exchange with feasible neighbors for cooperative tracking. Moreover, the cyber-twin model can make UAVs coordinate remote cooperators based on a rough topology relationship of remote UAVs for cooperative tracking. The rough topology, including positions and connectivity among UAVs, can be acquired in real-time by a distributed routing algorithm [26]. The designed cyber-twin system is divided into three parts:

1) Heterogeneous data sensing and processing.
2) Information management and exchange.
3) UAV swarm cooperation.

Heterogeneous Data Sensing and Processing: The operation is implemented in the physical tracking scenario. We utilize an onboard camera and vision sensor to capture and recognize targets for successful target detection. Both targets and trackers can be significantly distinguished based on lightweight YOLOv5 architecture [27]. In this case, the images of targets captured by onboard cameras is processed based on a Convolution Neural Network (CNN) algorithm. The training dataset is manually prepared by frequently capturing our given targets in the real world. Furthermore, we download many similar-sized target images and tracker images from Google Chrome explorer to improve the training reliability of the neural network.

We utilize the stochastic gradient descent method to train our detection model with a batch size of 32 images. The updated weight κ of the loss function L and relevant momentum variable φ are given by

$$\kappa_{a+1} = \kappa_a + \varphi_{a+1}, \tag{1}$$

$$\varphi_{a+1} = 0.9 \times \varphi_a - 0.0005 \times l_a \kappa_a - l_a \Big(\frac{\partial L}{\partial \kappa_a} \Big), \tag{2}$$

where a is the iteration index; l_a is the corresponding learning rate; $\frac{\partial L}{\partial \kappa_a}$ is the average over the ath batch of the derivative of the loss function $L(X) = -\log P(X|\hat{X}_i)$ with respect to κ_a, where X is the inputted image representation; $\hat{X}_i$ is the ith type of image representation.

Once the output of CNN tells us that the manners of vehicles (targets) are illegal, UAVs can acquire the relevant status of targets, including physical distances, positions, and mobile velocities, based on Ultra-WideBand (UWB) radio. With the assumption of no other physical interfere, UWB can rapidly scan surrounding mobile objects with 4.3 GHz center frequency [28]. UAVs can control the UWB to transmit pulse using Binary Pulse Position Modulation

$$s_i(t) = \sum_n b_n \delta(t - c_n I_l - n I_s), \tag{3}$$

TABLE 1
List of Used Main Notations in This Work

Notation	Description
$\mathcal{M}$	Set of UAVs
$\mathcal{K}$	Set of mobile targets
ρ	Successful tracking ratio of UAV swarm
$r_{i,j}$	Transmission ratio between UAV i and j
E_i^s	Energy consumption in sensing for UAV i
t_i^s	Sensing latency of UAV i
$E_{i,j}^c$	Energy consumption in communication
$t_{i,j}^c$	Communication latency between UAV i and j
Λ_k	The maximal acceptable prediction error for target k
E_i^f	Flight energy consumption of UAV i
$d_{i,j}$	Flight physical distance between UAV i and j

where $s_i(t)$ is the transmission signal of UAV i at time slot t; b_n is the polarity of pulses; c_n is transmission symbol; I_l and I_s are the length of time slot and symbol duration, respectively. The subscript n denotes the nth scan subarea. Numerous signals s_i composing a three-dimensional beam transmit to diverse directions for acquiring the velocities and mobile directions. In a practical scenario, we test a UWB device with a 30° scan angle. Based on the round-trip time of signals t_g and relative transmission angle $\theta(s_i)$ obtained by the Reconfiguration and Evaluation Tool (RET), the mobile velocity v_k of target k in time $t(I_l)$ is $v_k = \frac{1}{C}\sum_{t_g=1}^{C} \Delta \frac{c \times t_g}{2\Delta I_l}$, where c is electromagnetic ware velocity; $\Delta(x)$ is the difference value. After that, the *data processing operation* is implemented to improve the accuracy of the target estimation. The final output value O_p from heterogeneous sensors is fused based on a weighted mean method

$$O_p = \frac{1}{W}\sum_{w=1}^{W} \omega_w p_w, \tag{4}$$

where W is the number of embedded sensors; ω_w is the weight of sensor w; p_w is the estimation value of sensor w. Based on this, the sensing performance ω_t can be given with a predefined threshold ϖ [29]

$$\omega_t = \frac{\sum_k \mathrm{Nu}[\mathrm{Surf}(t, S_i)]}{K} \geq \varpi, \tag{5}$$

where $\mathrm{Nu}[\mathrm{x}]$ is the number of targets in the valid areas with sensed mobile targets; $\mathrm{Surf}(t, S_i)$ is the non-overlapping surface sensed at time slot t by UAV i with state S_i embodied in Section 5. Then, the cumulative successful tracking ratio ρ can be given as

$$\rho = \lim_{T\to\infty} \frac{1}{T}\sum_{t=0}^{T} \omega_t. \tag{6}$$

Information Management and Exchange: Instead of the raw analog signals, we process the data to obtain analyzable information terms for information management in the virtual world. Explicitly, the cyber-twin models are able to assist UAVs in predicting mobile trajectories of surrounding targets based on the processed data for accurate tracking. Furthermore, the cyber-twin models can assist UAVs in time synchronization which is essential in the distributed pattern. The local time clock is updated when events (like sensing and exchange) are triggered. The Lamport timestamp algorithm is invoked to determine the order of events for the distributed time synchronization [30]. In concrete, the exchanging information composing a set of information items is stored in the cache of UAVs. Each item is embodied with an attribute set $a_i = \{o_j(c_j, m_j), o_k(c_k, m_k)\}$, where o_j and o_k are the status of neighbor j and sensed target k as detailed in Section 5; c_j and m_j are the collection and storage time with local timestamp f_i, respectively. The timestamp can be exchanged to ensure synchronous communication among UAVs. For the exchange between any two UAVs, the cyber-twin model can conduct UAVs to set their local clock f_i and f_j to be equal to the largest value. It is arranged and distributed by a center before the MTT implementation

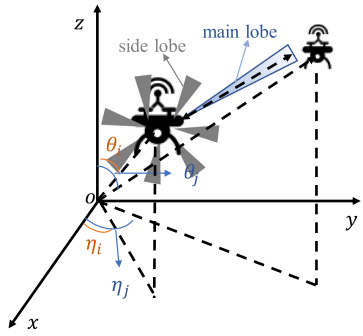

Fig. 4. Illustration of communication using beamforming among UAVs.

with symmetry of synchronous information exchange. The cyber-twin model can assist the UAV i on sending back a dummy message with its local clock value f_i to UAV j. UAVs can adjust their local clocks that can alleviate the deadlock as long as UAVs adhere to the rule. The comparison between the two timestamps is given by

$$a_i \rightarrow a_j, \quad if \quad (f_{a_i}[i] \leq f_{a_j}[i]) \wedge (f_{a_i}[j] < f_{a_j}[j]), \tag{7}$$

where $f_{a_i}[i] \leq f_{a_j}[i]$ denotes that UAV j has received a clock value from UAV i at least as recent as the execution of a_i. Meanwhile, a_j is transmitted to UAV j after a_i; $f_{a_i}[j] < f_{a_j}[j]$ implies that UAV i does not have the up-to-date information of UAV j. We can realize the synchronization between any two UAVs after the event-trigger operation. The information is also updated in real-time by the event handler component, which will be implemented when the positions of the targets and neighbors change.

For the information exchange, the cyber-twin model can use multiple antennas and beamforming technologies. In Fig. 4, the elevation angles of UAV i and j are denoted as θ_i and θ_j, $\theta \in [0, \pi]$. The azimuth angles are respectively represented as η_i and η_j, $\eta \in [-\pi, \pi]$. The array factor κ can be dynamically modulated by the cyber-twin model

$$\kappa(\eta, \theta, I) = \sum_{a=1}^{A} I_a \exp^{-j\frac{2\pi}{\lambda} d_a(\eta_i, \theta_i)} \exp^{j\frac{2\pi}{\lambda} d_a(\eta_j, \theta_j)}, \tag{8}$$

where A is the number of antennas of each UAV; λ is the wavelength; I is the current normalized excitation weight limited in [0, 1].

The directions of beams can be dynamically changed with θ and η. Due to the spatial sparsity of the transmission channel, it is common to abstract the actual array beam pattern for each beam with a constant main-lobe over the beamwidth and a constant side-lobe [31]. Let $G_{\mathrm{ma}}(A)$ and $G_{\mathrm{si}}(A)$ denote the gains of the main lobe and the side lobe, respectively. $G_{\mathrm{ma}}(A)$ is assumed to be non-decreasing while $G_{\mathrm{si}}(A)$ and beamwidth are non-increasing [32]. In this case, the ratio $\frac{G_{\mathrm{ma}}}{G_{\mathrm{si}}}$ is non-decreasing. Based on the assumptions and the conditions on network geometry, the transmission model with Line of Sight (LoS) propagation between UAV i and j under a given relative physical distance $d_{i,j}$ is represented as

$$r_{i,j} = B(A)\log_2\left(1 + \frac{a_i^{f_i} P_{\mathrm{total}} G_{\mathrm{ma}}(c_i) \hat{e} d_{i,j}^{-\alpha}}{\hat{T} + \bar{T} + a_i^{f_i}\sigma^2}\right), \tag{9}$$

where $\hat{T} = \sum_{l_j \in \hat{\Omega}} G_{\text{ma}}(c_j) L(l_j) e_j$ is the interference received from UAV i with beams pointing towards the UAV j; $L(x)$ is captured channel gain function with spatial distribution density x of UAVs; $\bar{T} = \sum_{c_j \in \bar{\Omega}} G_{s_j}(c_j) L(l_j) g_j$ is the interference with beams pointing away from the UAV j; $\hat{\Omega}$ and $\bar{\Omega}$ are sets of interfering UAV j in the sight of main lobe and side lobe, respectively. $\hat{e}$, e_j, and g_j are random variables capturing the small scale fading of the link $a_i^{f_i}$, interfering links with beams pointing towards the UAV j, and away from the UAV j, respectively; $B(A)$ is the channel bandwidth; P_{total} is the total transmission power of A antennas; $d_{i,j} = \sqrt{(x_i - x_j)^2 + (y_i - y_j)^2 + (z_i - z_j)^2}$ is the physical distance between the two UAVs; $G_{i,j}$ is the transmission gains; $a_i^{f_i} \in \{0, 1\}$ is the assigned channel index with spectrum f_i; $u_{f_i,f_m} = 1$ with $f_i - f_m = 0$ denotes that two UAVs simultaneously occupy the same channel while $u_{f_i,f_m} \to 0$ with $(f_i - f_m) \to \infty$ implies that the channel f_i and f_m are sufficiently separated with $u_{f_i,f_m} \in (0, 1]$; $\sigma \sim N(0, \delta)$ is the zero mean Gaussian random variable with a standard deviation of δ.

UAV Swarm Cooperation: During the tracking process, the cyber-twin models can coordinate both proximal UAVs and remote UAVs for accurate MTT. In addition, the cyber-twin model can provide feasible tracking paths with collision avoidance to ensure a low-latency MTT. The cyber-twin model can assist UAVs in inviting suitable neighbors for proximal cooperative tracking. It can reduce the communication overhead with small numbers of neighbors involved. In this case, the cyber-twin model can also acquire feasible associations among UAVs and moving targets for a highly successful tracking ratio based on the low-latency information exchange. For remote cooperation, the cyber-twin models can assist UAVs in exploring feasible relays implementing remote information delivery for accurately tracking high-speed moving targets. It can reduce the data transmission latency by seeking short-distance information delivery paths. The specific cooperative tracking scheme is presented in Section 5.

4 Problem Formulation

Based on the designed framework in Section 3, an optimization model for MTT is formulated to explore the optimal communication and sensing manners in this section.

In the conventional distributed tracking pattern without cyber twin's support, UAVs cannot always select feasible cooperators in real-time to implement cooperative tracking due to the high mobility of both UAVs and moving targets. In this case, the probability of tracking failure and communication overhead in a swarm might increase with frequent information exchange in a large-scale MTT scenario. The system energy consumption might also increase with long tracking paths due to unreasonable associations among UAVs and moving targets. To formulate the problem with optimization of communication efficiency while ensuring a highly successful tracking ratio for a long-term tracking process. The cyber-twin model can accurately estimate neighbor states to alleviate energy consumption and latency in communication for real-time tracking.

4.1 Sensing and Communication Analysis

We can acquire different types of data from onboard sensors with different collection rates. It brings into energy consumption in sensing by scheduling onboard sensors

$$E_i^s = \sum_{w=1}^{W} \beta_w b_{i,w}^k \alpha_{s,w} q_{i,w}^k, \tag{10}$$

where $\alpha_{s,w}$ is overhead (Joule) of sensing a bit of data from sensor w; $q_{i,w}^k$ is the corresponding data size (bits); β_w denotes the collecting rate; $b_{i,w}^k \in \{0, 1\}$ represents whether the sensing link exists. The corresponding latency overhead t_i^s with the sensing rate λ_w is given by

$$t_i^s = \sum_{w=1}^{W} \frac{q_i^w}{\lambda_w}. \tag{11}$$

For the wireless information exchange among UAVs with unreliability, we consider the data re-transmission with the Automatic Repeat Query (ARQ) scheme [33]. The information exchange between UAV i and j is estimated based on the energy consumption in communication. It is defined as the transmission energy consumption in one unit of time between UAV i and j. We define a package with a fixed size l_p (bits) is exchanged among UAVs. We consider the data re-transmission with the Automatic Repeat Query (ARQ) scheme [33]. We assume that transmission power is P_r. The power consumption $\hat{P}$ is computed as $\hat{P} = P_r I$, where I is a variable denoting the number of re-transmissions. The energy consumption in communication $E_{i,j}^c$ between UAV i and j is presented as

$$E_{i,j}^c = q_{i,j} l_p \hat{P} T_r, \tag{12}$$

where $q_{i,j}$ is the number of packages from UAV i to UAV j; T_r denotes a requested time. In this case, the number of re-transmission I is computed as $I = \sum_{R=1}^{\infty} R(1 - p_{\text{re}}^R) p_{\text{re}}^{-p_{\text{re}} R(R-1)}$, where R denotes that the Rth transmission is successful; p_{re} denotes the re-transmission probability. The corresponding latency overhead $t_{i,j}^c$ is written as

$$t_{i,j}^c = q_{i,j} l_p T_r I, \tag{13}$$

where $T_r I$ denotes the transmission time of a bit for each information exchange.

4.2 Trajectory Prediction

Based on the obtained information from the sensors, UAVs need to predict targets' trajectories. However, many conventional inertia prediction approaches such as the Kalman Filter algorithm are infeasible for these targets with random mobile trajectories. The predictive error is accumulated as time increases which can cause the tracking failure. In the MTT network, Extend Kalman Filter method as a practical approach is used to cope with the nonlinear mobile targets [34], [35]. It can approximate the nonlinear motion to linear motion based on the Taylor series methodology.

The EKF method is composed by *prediction* and *update* processes. *In the prediction stage*, the initial coordinate of the UAV i is formulated as $x_{t+1|t} = F x_t + \omega_t$, where F is transfer matrix; ω_t is standard Gaussian White noise. The prediction is evaluated based on $P_{t+1|t} = F \times P_t \times F^T$. The estimation

is fed into *the following update stage*. A covariance function $S_{t+1} = P_t + H_{t+1}P_{t+1|t}H_{t+1}^T$ is defined to acquire the Kalman gain $K_{t+1} = P_{t+1|t} \times H_{t+1}^T \times S_{t+1}^{-1}$, where H is the measurement matrix. The updated coordinate is then represented as $x_{t+1} = x_{t+1|t} + K_{t+1}\widetilde{y}$, where $\widetilde{y}$ is measurement residual (i.e., the difference between the measurement value and the evaluation value). The error of the UAV i is defined as $\alpha_i^k(t) = (x_t - x_{t|t-1})$. The system prediction error constraint is given with the maximal acceptable error Λ_k

$$\frac{1}{M}\sum_{i=1}^{M}\alpha_i^k(t) \leq \Lambda_k, \tag{14}$$

4.3 Objective Formulation

From the above analysis, the average energy consumption for sensing and communication is constrained by

$$\frac{1}{T_i}(\sum_j \varrho_{i,j}E_{i,j}^c + E_i^s) \leq E_{i,\max}, \tag{15}$$

where $\sum_j \varrho_{i,j} = 1$, $\varrho_{i,j} \in \{0,1\}$; $E_{i,\max}$ denotes the maximal available budget of UAV i in a unit time. T_i is the consumed time of UAV i for target sensing and neighboring communication. The constraint of latency overhead is given by

$$\sum_j \varrho_{i,j}t_{i,j}^c + t_i^s \leq t_{i,\max}, \tag{16}$$

where $t_{i,\max}$ is the maximal latency deadline. Based on Eq. (9), the communication efficiency is written as

$$\vartheta_i^e = \frac{\varrho_{i,j}r_{i,j}}{P_{\text{total}}P_{\text{circ}}}, \tag{17}$$

where P_{circ} is the circuit power consumption. Except for the energy consumption in communication, the energy consumption of flight and hovering needs to be analyzed to improve MTT capability. The consumed power is directly related to the velocities of UAVs [36]. The energy consumption of flight of UAV i is given by

$$E_i^f = \int_{t-1}^{t} P_i^f(\|v(s)\|)ds, \tag{18}$$

where $P_i^f(\|v(s)\|)$ is the power with velocity $v(s)$; $\|v(s)\|$ is the UAV speed at time instant s with $s \in [t-1, t]$. The hovering consumption is also related to aircraft type and air density ρ_a. The corresponding consumption is written to

$$E_i^h = \int_{t-1}^{t} \frac{c_d}{8}\rho_a A v_a^3 R_a^3 + (1+c_a)\frac{N_w^{3/2}}{\sqrt{2\rho_a A}}ds, \tag{19}$$

where c_d is profile drag coefficient; ρ_a is air density (kg/m^3); A and v_a are rotor disc area (m^2) and blade angular velocity (radian/seconds) respectively; R_a and c_a are rotor radius (m) and incremental correction factor, respectively; N_w is weight of UAV i (Newton). However, the two status cannot simultaneously enable for UAV i, the non-energy consumption in communication E_i^{nc} is given by

$$E_i^{\text{nc}} = \max\{E_i^f, E_i^h\}, \tag{20}$$

where $E_i^f = 0$ when UAV i hovers, and vice versa.

Thereafter, the optimization model is formulated as

$$P1: \max\left\{\lim_{T\to\infty}\frac{1}{T}\sum_{t=0}^{T}\left[\sum_{i=1}^{M}(\vartheta_i^e - E_i^{\text{nc}})\right]\right\}$$
$$\text{s.t.}\begin{cases} C1: (5),(14),(15),(16), \quad i,j \in \mathcal{M} \\ C2: \varrho_{i,j} \in \{0,1\}, \\ C3: r_{i,j} \geq r_{\min}, \\ C4: d_{i,j} \geq d_{\min}, \\ C5: v_i \leq v_{i,\max} \end{cases} \tag{21}$$

where $C1$ denotes the constraints of sensing capability, systematic budget, and relevant latency; $C2$ gives that UAV i can simultaneously associate a neighbor in same slot t; $C3$ is the constraint of transmission rates; $C4$ gives the minimal flight distance among UAVs for collision-avoidance. $C5$ denotes that the maximal tracking speed constraint for each UAV. Based on the cyber-twin model, the given constraints can tightly restrain the formulated objective. For example, UAVs will find optimal cooperators to communicate for cooperative tracking if the cyber-twin model can provide accurate trajectory prediction of targets with the prediction accuracy constrain. The problem is NP-Hard based on a given proof in Appendix, which can be found on the Computer Society Digital Library at http://doi.ieeecomputersociety.org/10.1109/TMC.2022.3193499.

5 ISC-Enabled UAV-MTT

In this section, we present our integrated sensing and communication (ISC) enabled distributed tracking algorithm to realize low-overhead UAV-MTT in a cyber-twin system. We decompose the NP-Hard problem into two sub-problems with topology control for clear analysis.

5.1 UAV Swarm Cooperation

In MTT, the topology control is quite important for cooperative tracking. The position and topology of UAVs have a significant impact on cooperative sensing. The spatial physical distance among UAVs influences coverage of target sensing areas and communication efficiency. Furthermore, it can indirectly affect the building of cyber-twin models due to dynamic topological relationships.

In this context, we give a distributed topology control rule for collision avoidance, accurate sensing, and efficient communication. To efficiently control the topology, we set a safe physical flight distance constraint $d_{\min}$ to ensure physical flight safety. With the prerequisite and the challenge of undetermined trajectories of targets, UAVs can exchange information with neighbors among the communication distance. When the neighbors change positions to associate multiple targets simultaneously for a highly successful tracking ratio, UAVs can implement low-latency information exchange within a 2-hop communication distance in the neighborhood. The exchanged information queue $Q_{i,t}$ of UAV i has three parts:

1) The received information $y_{i,t}$ that is forwarded to other UAVs at time slot t.
2) The received information $x_{i,t}$ from neighboring UAVs that will not be forwarded at time slot t.

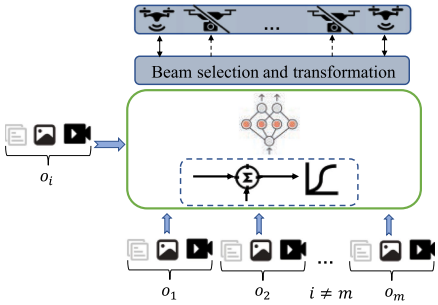

Fig. 5. Illustration of ISC-enabled neighboring cooperation.

3) The self-sensed information $z_{i,t}$ at time slot t.

The queue update is written as

$$Q_{i,t+1} = \left[Q_{i,t} - \sum_k (x_{i,t}^k + y_{i,t}^k) \right]^+ + \sum_k z_{i,t}^k, \tag{22}$$

where $[x]^+ = \max\{0, x\}$.

ISC-Enabled Neighboring Cooperation: With the real-time communication approach, cyber-twin models can assist UAVs in acquiring precise topology information of adjacent UAVs and rough topology relationships of remote UAVs. The precise topology information includes positions of UAVs, associations among UAVs, and postures of UAVs. It can assist UAVs in accurately estimating neighboring states for cooperative tracking. Based on the neighboring observation, we invoke an attention-based model to explore optimal neighbors for information exchange based on predicted targets' trajectories. Explicitly, the neighboring attribute $o_{i,j}^t$ is trained by a Multiple Layers Perception (MLP) network shown in Fig. 5. Wherein, an encoder-decoder architecture is designed based on deep learning manner [37]. For the encoder operation, observations of UAV i, $h_i^t = (h_{i,1}^t, h_{i,2}^t, \ldots, h_{i,m}^t)$, are inputted to the MLP network. The original state space is mapped into a feature space with a lightweight conversion operation $h_{i,j}^t = f(o_{i,j}^t, W_{i,j}^k)$, where $W_{i,j}^k$ is a weight value. The decoder operation can be implemented by the activation function $m_i^t = o_i^t W_{i,j}^q$, where $W_{i,j}^q$ is a hyper-parameter. We can use $\tanh$ function to obtain the communication probability between UAV i and its neighbor j, where $e_{i,j}^t = \tanh(m_i^t h_{i,j}^t)$. UAV j is selected if $e_{i,j}^t \geq 0$; and vice versa.

ISC-Enabled Remote Cooperation: The rough topology information includes positions of UAVs and associations among UAVs. This topology information is obtained in real-time by a distributed routing algorithm [26] and stored as a graph presentation in the cyber-twin model. The cyber-twin model can provide a directional information delivery service based on the rough topology information and predicted trajectories of targets. Explicitly, the cyber-twin models can assist UAVs in selecting feasible neighbors as relays to deliver information towards the predicted directions of target trajectories. The relay UAVs will feed back self-information to the last-hop UAV for delivery state acquisition. We discuss the delivery state from two perspectives.

1) The remote cooperators are available with a received feedback information in a given threshold time.
2) UAVs cannot get the feedback information from the remote cooperators in the threshold time.

Algorithm 1. UAV Swarm Cooperation

// **Definition:** $E_{\max} = 1000$.
//**neighboring cooperation:**
Input: Number of hidden layer H; training epochs $E_{\max}$; observation information o; number of neighbors m; threshold value ε.
Output: Communication neighbor vector $C^{M\times 1}$.

```
Construct MLP network with H hidden layers
while E ≤ E_max do
  Initialize observation o_{i,j}^t
  for each UAV i do
    Compute the encoded representation h_i^t.
    for each neighbor of each UAV do
      Compute the important degree h_{i,j}^t
      Compute the attention m_i^t
    end for
  end for
end while
//remote cooperation:
if d_{j,v} ≥ d_com then
  Implement the shortest path approach mentioned in Section 5.1
end if
if d_{j,v} < d_com then
  Initialize the distance estimation information C_d
  for each UAV i do
    for each target k do
      if i sense k then
        while C_d > ε do
          for each neighbor from m do
            Compute the angle θ
            Select the neighbor with the minimal angle to forward the information
            Update the C_d using Eq. (23) and relay UAV
          end for
        end while
      end if
    end for
  end for
end if
```

For the first case, multiple candidates of remote cooperators may be found based on the directional delivery approach. The cyber-twin models can compute physical distances from where targets are approaching and exchange the information with other candidates. The optimal cooperator with the shortest physical distance is selected to implement standby tracking. The second case implies that the current UAVs cannot find feasible next-hop relays for smooth delivery. The cyber-twin models can still conduct UAVs to autonomously exchange the physical distances from target positions with other relays. The optimal UAV with the shortest distance will fly to the assigned airspace for standby tracking. It significantly reduces communication overheads supported by the topology information in cyber-twin models. The delivery routes can be shorten to $\frac{C_d}{d_{\text{com}}}$hops at least under a given communication range d_{com}. The information feedback operation can also assist UAVs in acquiring a lightweight cyber-twin model with neighbor observation. Consequently, the cyber-twin model easily

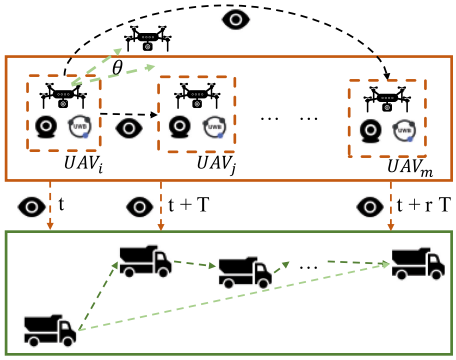

Fig. 6. Illustration of ISC-enabled remote cooperation.

control the topology for cooperative tracking by selecting optimal cooperators.

Based on the topology information known by cyber-twin models, we discuss the remote cooperation from the perspective of the ISC:

1) The sensing range is larger than communication range.
2) The communication range is larger than or equal to sensing range.

As shown in Fig. 6, UAV i can predict mobile trajectory of target k over a period of time (from t to $t+rT$) based on Eq. (14). The aqua dotted-line represents the mobile direction of target k, and the vector-distance is $d_{rT} = \sqrt{(x_t - x_{rT})^2 + (y_t - y_{rT})^2 + (z_t - z_{rT})^2}$. *When the sensing range is larger than the communication range,* UAV i can observe and discover the feasible remote cooperator m based on the vector distance. It is realizable to acquire positions and relative distances of all the relay UAVs with a wide vision. We can explore the shortest path from i to m to implement the information transmission. A connectivity matrix A^c is formulated to represent the dynamic topology relation. For UAV j and v, if physical distance $d_{j,v}$ acquired by onboard sensors (details in Section 3) is greater than the communication radius d_{com}, $A^c_{j,v} = 0$, and vice versa. The shortest transmission path with feasible relay UAVs is given based on the following steps.

S1 Set the origin UAV i and destination UAV m with the topology matrix $A_c = (V_c, E_c)$, where V_c and E_c are set of vertices and edges.
S2 Build set $\mathbb{S}_c = \{i\}$ and $\mathbb{U}_c = \{V_c\} \backslash i$.
S3 Select the relay v with the shortest distance $d_{i,v}$.
S4 Poll vertices with element 1 in the row of v.
  S4.1 Compute the physical distance $d_{v,j}$.
  S4.2 Update the distance as $d_{i,j}$ if $(d_{i,v} + d_{v,j}) > d_{i,j}$.
S5 Iterate S3 and S4 until all the relays are fed into $\mathbb{S}_c$; The shortest distance and relevant relays are recorded.

However, wide vision is unavailable when *the sensing range is smaller than the communication range.* In this case, UAVs can implement remote cooperation by selecting feasible neighbors as relay UAVs with the minimal angle θ in Fig. 6, where θ is the angle between the information forwarding direction and the mobile direction of the target k. Meanwhile, a distance estimation value C_d is defined to record the current transmission distance for efficiently interrupting the transmission when $C_d \leq \varepsilon$, where ε is a given threshold. The C_d is updated by

$$C_d = C_d - \|\overrightarrow{d_{i.j}} \times \overrightarrow{d_{rT}}\|_2, \tag{23}$$

where $C_d = d_{rT}$ is the initial distance estimation; $x \times y$ is the projection of x onto the y with cross-product operation; $\|z\|_2$ denotes the euclidean norm; $d_{i,j}$ is the physical distance between UAV i and the next hop j. The details are given in Algorithm 1

Algorithm 2. ISC-Enabled Tracking for UAV-MTT

// **Definition:** $\gamma = 0.99 - 0.999$.
Input: Observation information S; Actor-critic network parameters θ^Q, θ^μ; updated weighted γ;
Neural network parameters θ^P and θ^a; replay memory $\mathcal{R}$; neighboring set of UAV i m_i; Number of antennas A.
Output: The mission execution decision.

```
Set the number of agents M
for each episode in all rounds do
  Set an initial action μ and receive the relevant state
  for each time slot t do
    while M ≠ ∅ do
      for each neighbor of UAV i do
        Implement Algorithm 1, and M = M\{m_i}
      end for
    end while
    Select an action and obtain the reward R_{i,t}
    Store the experience to R
    Sample a min-batch to evaluate
    for each sample do
      Compute the new reward using Eq. (24)
      Compute Q-value using Eq. (25) and Eq. (29)
    end for
    Compute the loss gradients using Eq. (28)
    Update the gradients of neural network using
    Eq. (26) and attention network using Eq. (27)
  end for
end for
```

$$R_i(S_i, A_i) = u_i(S_i, A_i) - \frac{\alpha_i}{m_i}\sum_{i \neq j}\max(e_j(S_j, A_j) - e_i(S_i, A_i)) - \frac{\beta_i}{m_i}\sum_{i \neq j}\max(e_i(S_i, A_i) - e_j(S_j, A_j)) \tag{24}$$

$$\nabla_{\theta^\mu} J(\theta^\mu) = E_{S,A\backsim\mathcal{R}}\Big[\sum_i \nabla_{\theta^\mu}\mu(A_i|S_i)\nabla_{A_i}Q^\mu(S_i, A_i)|_{A_i=\mu(S_i)}\Big] \tag{25}$$

$$\nabla_{\theta^P} J(\theta^P) = E_{S,A\backsim\mathcal{R}}\Big[\sum_i g_i(P_i|C)\nabla_{P_i}\mu(A_i|P_i)\nabla_{P_i}\mu (A_i|P_i)\nabla_{A_i}Q^\mu(S_i, A_i)|_{A_i=\mu(S_i)}\Big] \tag{26}$$

$$L(\theta^a) = -\Delta\hat{Q}_i \log\left(p(P_i|\theta^a)\right) - (1 - \hat{Q}_i)\log\left(1 - p(P_i|\theta^a)\right) \tag{27}$$

5.2 ISC-Enabled Distributed Tracking

An ISC-enabled distributed tracking algorithm is proposed to improve sensing capability while reducing communication overhead (latency and energy consumption). Unlike

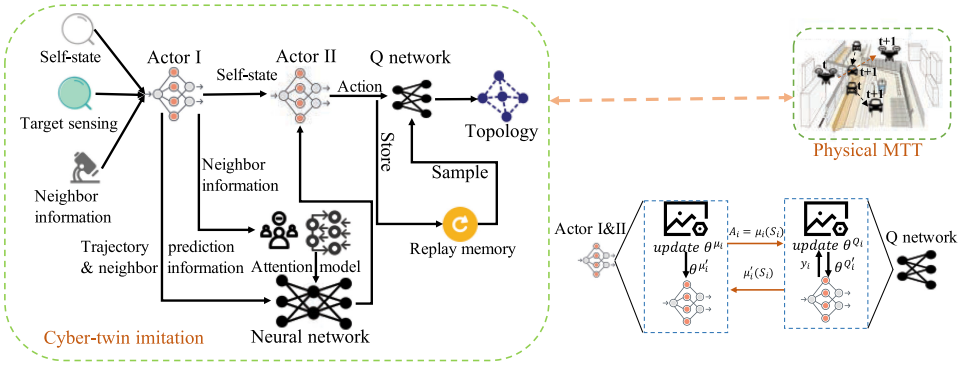

Fig. 7. Illustration of ISC based cooperative tracking networks in cyber-twin system.

some existing cyber-twin systems with frequent data collection, our system can realize the imitation synchronization between the virtual twin and the physical twin by only predicting mobile trajectories of sensed targets. It can significantly improve the synchronization performance without the target sensing latency. *In the physical world*, the freshest neighbor information is obtained based on the invoked Lamport time algorithm for advanced information exchanging (details in Section 3). When targets escape from the current sensing area, UAVs can exchange the information with their neighbors to transmit their following mobility status and the target information. The exchanging operation is event-triggered rather than periodicity. In this case, we also reduce the frequency of information collection from neighbors while ensuring the data's freshness.

In the virtual world, each UAV can make intelligent imitation with Multi-Agent Deep Deterministic Policy Gradient (MA-DDPG) architecture incorporating a policy network and a Q-network. The physical information is fed to the policy network to output corresponding actions. The actions are estimated in the Q-network. To obtain the optimal tracking cooperation policy, the process is qualified to a Stochastic Game (SG) problem with a tuple $\{\{S_i\},\{A_i\},\mathcal{T},\{R_i\}\}$, where $\{S_i\}$ is the state space of UAV i. It is noted that the S_i is dynamically updated because different targets and neighbors are sensed in the area of UAV i; $\{A_i\}$ is the corresponding action space; $\mathcal{T}$ is transfer function with $S_i \times A_i \rightarrow S_i$; $\{R_i\}$ is a reward function for a selected action. Note that we drop the time t in the following notations for simplicity. The S_i is divided into three categories:

1) Self-state: $s_i = \{\kappa_i, x_i, he_i, v_i, g_i, r_i, C_{i,t}, E^c_{i,j}, E^s_i\}$, where x_i, he_i, v_i, g_i are position coordination, flight height, flight velocity, and posture, respectively.
2) States of neighbors: $o_i = \{\{d_{i,j}\},\{h_j\},\{v_j\},\{g_j\}\}$, where $\{g_j\}$ is posture information of neighbor j, which is used to select neighbors for cooperative tracking.
3) State of targets: $\varpi_{i,k}$, the state of target k sensed by UAV i, including position, velocity, and posture.

The action space is $A_i = \{X_i, e_i, \{m_i\}, \{s_{i,j}\}, \{s^p_{i,j}\}\}$, where X_i and e_i are the flight position and pitch angle of UAV i; $\{m_i\}$ is the exchanged neighbor set for UAV i. The exchanged data types are represented as $\{s_{i,j}\}$ between UAV i and j with $\{s^p_{i,j}\}$ bits of exchanged data.

The sensing and communication are jointly optimized based on Eq. (21). Considering the energy consumption equilibrium in communication, the reward R_i is redefined by Eq. (24), where $u_i(S_i, A_i) = [\Delta E^s_i + \Delta E^c_i + \Delta t^c_i + \Delta C_{i,t}]$, and $\Delta[*] = *(t-1) - *(t)$. The temporal smoothed reward $e_j(S_j, A_j) = \lambda e^{t-1}_j(S_j, A_j) + u_j(S_j, A_j)$, and the parameters α_i and β_i can be respectively set as 5 and 0.05 [38].

As shown in Fig. 7, the architecture incorporates four components: critic module, actor module, neural network, and attention model, which are given as θ^Q, θ^μ, θ^P, and θ^a, respectively. The attention unit can connect to a hidden layer of the actor-I network. The sparse vector $C^{1\times m}$, where $C_j = 1$ denotes UAV i can exchange information with UAV j, is fed into the designed neural network. Then a matrix $P^{m\times\eta}$ is outputted based on observation information. The observation information and relevant actions are coupled to cache in the replay memory $\mathcal{R}$ with the tuples (S, A, R, S', C, P). The actions are defined by the designed action-value function based on the Bellman equation

$$L(\theta^Q) = E_{S,A,R,S'}\left[\sum_i (Q^\mu(S_i, A_i) - Y)^2\right], \tag{28}$$

where $Y = R_i + \gamma Q^{\mu'}(S_i, A_i)|_{A'_i=\mu'_i(S_i)}$; γ is the discount factor. The policy gradient is redesigned as Eq. (25). Based on the chain rule, the parameters of neural network are updated by back-propagation operation with Eq. (26), where $g_i(*)$ denotes the communication group of UAV i. The parameters are updated as $\theta' = \tau\theta + (1-\tau)\theta'$. The estimation error is computed by

$$\Delta Q_i = \frac{1}{\|C\|}\sum_j Q(S_j, A_j|\theta^Q) - \sum_j Q(S_j, \bar{A}_j|\theta^Q), \tag{29}$$

where $\bar{A}_j$ is the action under the soft-communication pattern. The update is represented in Eq. (27). The algorithm is detailed in Algorithm 2. The proof of our algorithm convergence is presented in Appendix, available in the online supplemental material.

5.3 Algorithm Complexity Analysis

For our algorithm, the computational complexity is analyzed based on four parts. The complexity proof with specific derivations is given in Appendix, available in the online supplemental material.

First, the complexity of the trajectory prediction algorithm is $O(n^2)$, where n is the number of rows based on an iteration manner [39]. Second, the time complexity of the

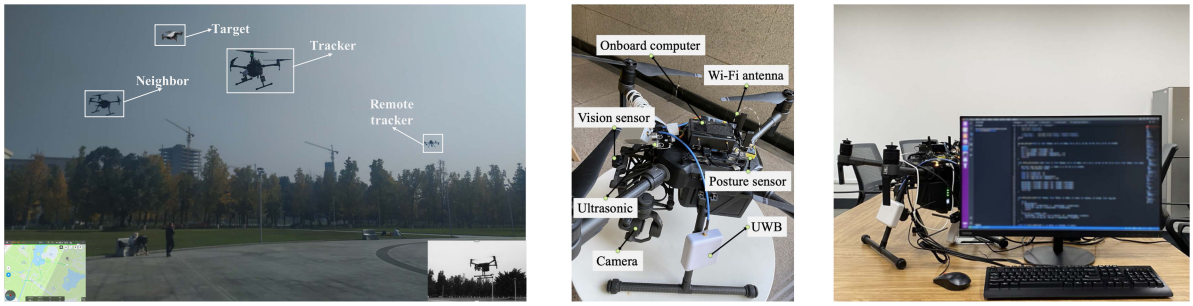

(a) Snapshot of target tracking. (b) Onboard sensors. (c) Data processing and training.

Fig. 8. The cooperative tracking scenario is represented in Fig. 8a. The observation of tracker is given at the right bottom and the trajectory of target is shown at the left bottom. The data is obtained by off-the-shelf sensors represented in Fig. 8b. The data is processed in Fig. 8c.

ISC-enabled neighbor cooperation is $O(I^2\ d)$, where I is the number of iterations of the designed neural network; d is the number of dimensions of vector $h_{i,j}$. In addition, the time complexity of the remote tracking cooperation is $\max\{O(\frac{V_c^2}{2}-\frac{1}{2}+E_c), O(n^2I^2\ d)\}$. Finally, the time complexity of the ISC-based distributed tracking algorithm is given by $O(BT)$, where B is the iterative number of episodes in Algorithm 2; T is the number of time episodes. Thereafter, the total complexity of the proposed algorithm is represented as $O(BT)\max\{O(\frac{V_c^2}{2}-\frac{1}{2}+E_c), O(n^2I^2\ d)\}$. The complexity is lower than traditional deep reinforcement learning due to selecting the partial neighbors to share with instead of all UAVs.

6 Performance Evaluation

In this section, we simulate our proposed tracking cooperation algorithm in Python using the data collected from real testbeds on the campus of the University of Electronic Science and Technology of China (UESTC). The UAV-MTT system includes both hardware and software implementations. We evaluate the sensing and communication performances with different numbers of UAVs and mobile targets. We will open our source code and share sensors' data on GitHub.

Hardware: We randomly plan multiple trajectories of mobile targets based on the DJI GO 4 APP. The flight trajectories are stored in the cache for the tracking imitation. For the trackers, as shown in Fig. 8b, there are mainly four components: a small-size Manifold computer with computing-intensive NVIDIA Jetson TX2 GPU module to construct our cyber-twin system with required data for cooperative tracking imitation, a GPS acquiring geographical positions, WiFi modules enabling communication with neighbors, and onboard sensors obtaining the information of neighbors and targets (detailed in Section 6.1).

Software: We choose UAVs as the mobile targets for a challenging MTT. In the scenario, multiple trackers and targets are deployed in a boundary area with $3000\ m \times 3000\ m$. In each small enough time slot t, the positions of UAVs and targets are assumed to be constant. All the information collected from the real world is fused based on an deep learning model [40]. The processed data for training runs in the Manifold. The training process is implemented offline using the Pytorch architecture and Python 3.7. In addition, the DJI onboard software development kit is developed to obtain the targets' postures in the lightweight YOLOv5 architecture.

We use five benchmark algorithms for comparison.

1) *Deep Reinforcement Learning (DRL) based multi-agent communication scheme* [41]: It enables the communication among agents based on the double attention model to reduce the redundancy of messages.
2) *Existing Integrated Sensing And Communication (ISAC) based scheme* [42]: It adjusts the antenna array to optimize sensing and communication performance only based on the Radar device.
3) *Conventional DDPG scheme in a distributed pattern* [43]: It coordinates UAVs to track targets using the framework of centralized training with decentralized execution.
4) *Non-cooperative tracking scheme:* Here we replicate our algorithm except for the remote cooperation.
5) *Deep Q-learning based multi-agent communication* [44]: It utilizes deep Q-learning to learn communication protocols for information exchange among agents.

6.1 Data Collection

We randomly deploy multiple targets and UAVs in an area of interest on our UESTC campus. The UAVs can observe targets and neighbors during the tracking process. The observation mentioned in Section 5 can be divided into four parts: 1) the status of neighbors and targets obtained from vision sensors; 2) the velocities of targets and neighbors from UWB sensors; 3) the posture information from camera and vision sensors with lightweight YOLOv5 architecture [27]; 4) mobile trajectories of targets manually planned by DJI pilot APP.

The cooperative MTT operation is shown in Fig. 8a. UAVs can observe the status of neighbors and discover mobile targets flying in their sensing ranges. All the utilized onboard sensors are shown in Fig. 8b. The vision sensor and camera are utilized to capture the targets. The ultrasonic and UWB sensors can acquire the positions and velocities of targets. The postures of UAVs are real-time measured for efficient sensing based on the posture sensor. The collected information from these heterogeneous sensors is conveyed to the UAV CPU based on serial port protocols, where the data processing is realized and visualized in Fig. 8c. The swarm cooperation is evaluated by the following simulation results. The main parameters are summarized in Table 2.

TABLE 2
Simulation Parameters

Parameter Description	Value
Number of UAVs	[5, 30]
Number of mobile targets	[10, 60]
The maximal tracking velocity of UAVs	56 km/h
Average moving velocity of the targets	[32 km/h, 90 km/h]
Total tracking area	3000 m $\times$ 3000 m
Pitch angle of the UAVs	$[-130^{\circ}, +40^{\circ}]$
Number of antenna of each UAV	4
Learning rate	[0.001, 0.009]
Transmission power	[60 mW, 80 mW]
Communication bandwidth	[50 MHz, 100 MHz]
Minimal safe flight distance of the UAVs	3 m
Average sensing rate of the UAVs	1 MByte/s
Horizontal sensing distance of the UAVs	[0 m, 30 m]
Gaussian White Noise	-96 dBm/Hz
The acceptable system response latency $t_{i,\max}$	1.5 seconds

6.2 Evaluation Results

In this subsection, we evaluate the performance of the MTT system using some key metrics. We summarize the metrics and give the evaluation results to verify our system qualitatively and quantitatively.

Obtained Reward: In the learning process based on our proposed algorithm in Section 5, R_i is determined by some hyper-parameters: learning rate l, discount factor γ, and sampling batch size b_s. As shown in Table 2, the value l is adjusted from 0.001 to 0.009. We set a minimal step length of 0.0005 to explore the optimal l. Unlike the conventional setting method with constant γ, we use an event-trigger method to dynamically update γ in Eq. (28). The value γ is reduced when UAVs associate with other targets. The dynamic update can assist UAVs in forgetting the irrelevant historical tracking experience for enhanced learning performance. The batch size b_s is defined as 512.

Communication Consumption and Latency Overhead: The average energy consumption in communication of the MTT system is represented in Eq. (12). It is reasonable because the transmission probability between any two UAVs is equal. The value $q_{i,j}$ belongs to [8 MB, 10 MB] for transmitting image and context information. With six data re-transmissions based on IEEE 802.11 protocol [33], we obtain the maximal energy consumption in communication

$$E_{i,j}^{c} = 8 \times 10^{6} bits \times 0.08\ w \times 10^{-5} s = 6.4\ J. \tag{30}$$

We reduce the energy consumption in communication based on the following evaluation results with the proposed ISC method in UAV swarms. Similarly, the transmission latency among UAVs in Eq. (13) is reduced with the same $q_{i,j}$ for the real-time tracking requirement.

Sensing Performance and Successful Tracking Ratio: The sensing performance is defined in Eq. (5) with a threshold value $\varpi = 0.8$. We can acquire the number of sensed targets when learning performance reaches a convergence state. The successful tracking ratio is obtained based on Eq. (6) with a cumulative average ratio. The successful tracking ratio is larger than the sensing performance. This is because particle targets are captured in the next slot with our designed remote-tracking cooperation algorithm.

Fig. 9 shows the learning performance under the different number of UAVs and targets, where we mark the convergent gap between our algorithm and the fastest convergent benchmark. We can discover that our algorithm can perform the highest reward and robustness with which the communication efficiency is ensured to achieve cooperative tracking. On the other hand, the fastest convergence rate implies that our designed lightweight cyber-twin system is valid for real-time tracking. The conventional DDPG algorithm consistently performs the worst learning capability. The reason is that communication cannot be satisfied between any two neighbors with undetermined transmission interference and limited sensing ranges in practice. Our algorithm can on average improve the learning performance by over 11.5% compared to other benchmarks.

To estimate the performance of communication, Fig. 10a represents the comparison of energy consumption in communication on different numbers of UAVs. With 30 mobile targets, we can draw that all the energy consumption in communication can increase as the number of UAVs increases. It is because the frequency of information exchanges can increase for cooperative tracking. Compared to the benchmarks, our algorithm can significantly reduce energy consumption in communication with the designed attention model. The model can select the neighbors that fly in suitable physical positions. Our algorithm can reduce approximately 66.7% energy consumption in communication compared to the DRL-based algorithm.

Fig. 10b gives the comparison of latency overhead in the same scenario as Fig. 10a. All the latency overhead is increased when the number of UAVs increases. For the existing ISC-based algorithm, although communication performance can be optimized by tuning beams of antennas, the latency can still increase due to massive and redundant data collection. Our algorithm not only can realize adaptive beam adjustment but also can reduce redundant information exchange. Our algorithm can averagely reduce (72.2%, 80.9%, 85.7%, 87.2%) latency overhead compared to the DRL based, existing ISC based, Deep Q-learning based, and the conventional DDPG algorithm.

As illustrated in Fig. 10c, the performance of energy consumption in communication is analyzed based on the different number of targets. Under 20 trackers, the energy consumption in communication can increase with the number of tracked targets growing, but the increasing rate of our algorithm is the slowest one. The performance reveals that UAVs can still select the appropriate numbers of neighbors to exchange desirable information. Our algorithm can efficiently reduce (67.0%, 71.4%, 77.8%, 80.7%) energy consumption in communication compared to the DRL based, existing ISC based, Deep Q-learning based, and the conventional DDPG algorithm.

Fig. 10d compares the latency overhead in dynamic cases of the different numbers of randomly deployed targets. The number of UAVs is the same as Fig. 10c. Based on the prerequisite of accurate tracking, our algorithm can achieve low-latency communication. For our algorithm, the growing rate of latency overhead is moderate compared to the other

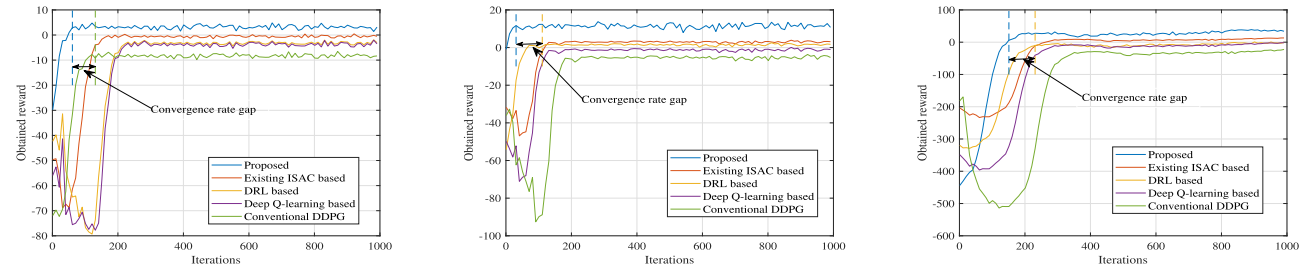

(a) 5 UAVs track 10 mobile targets. (b) 10 UAVs track 20 mobile targets. (c) 15 UAVs track 30 mobile targets.

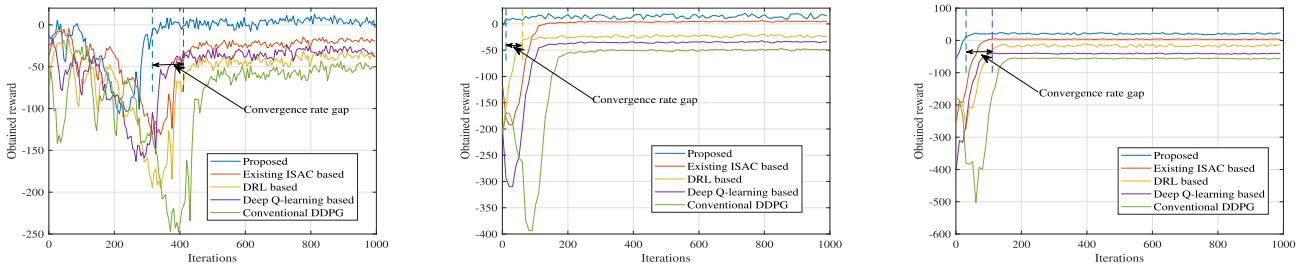

(d) 20 UAVs track 40 mobile targets. (e) 25 UAVs track 50 mobile targets. (f) 30 UAVs track 60 mobile targets.

Fig. 9. The comparisons of obtained reward are given under different numbers of UAVs and mobile targets.

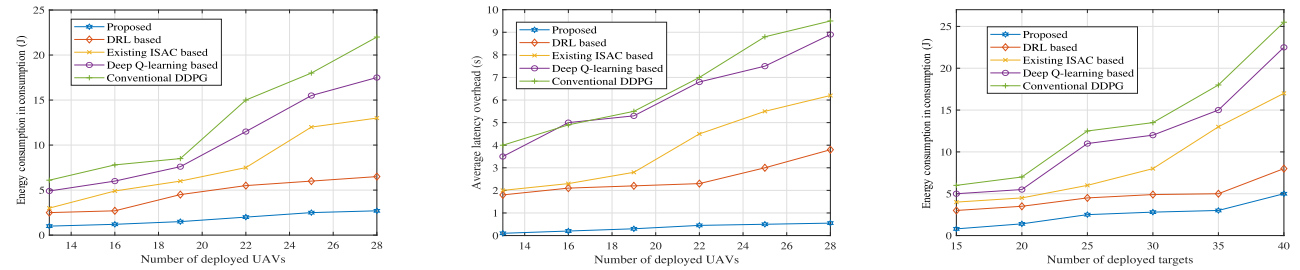

(a) Number of deployed UAVs vs. energy consumption in communication. (b) Number of deployed UAVs vs. latency overhead. (c) Number of deployed targets vs. energy consumption in communication.

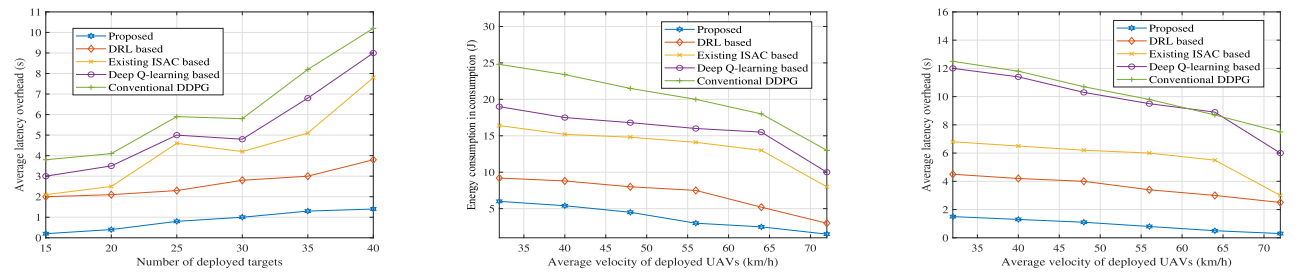

(d) Number of deployed targets vs. latency overhead. (e) Velocity of deployed UAVs vs. energy consumption in communication. (f) Velocity of deployed UAVs vs. latency overhead.

Fig. 10. The multidimensional performance evaluation for energy consumption in communication and latency overhead.

four benchmarks with the designed UAV swarm cooperative tracking service and lightweight cyber-twin system. It implies that our algorithm can efficiently coordinate UAVs to track different targets by exchanging a small quality of valuable information with partial neighbors. The information exchanging latency is significantly reduced by (52.3%, 75.0%, 82.1%, 83.3%) contrasting to the DRL based, existing ISC based, Deep Q-learning based, and the conventional DDPG algorithm.

Fig. 10e performs the energy consumption in communication based on the different velocities of 25 UAVs. The average speed of 50 mobile targets is 56 km/h. The energy consumption in communication decreases with the velocities of UAVs increasing due to the low frequency of remote cooperation operations. It is energy-wasting to explore multiple relays. However, our algorithm still achieves low-energy communication when the velocity of UAVs is significantly lower than that of targets compared to the benchmarks. It implies that our designed cyber-twin system can adaptively imitate the dynamic MTT to improve the tracking efficiency. The relevant overhead reduces by 81.25% contrasting to the existing ISAC-based algorithm.

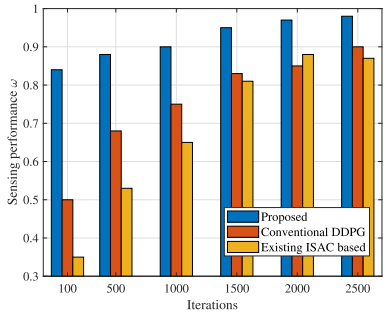

Fig. 11. Sensing performance vs. iterations.

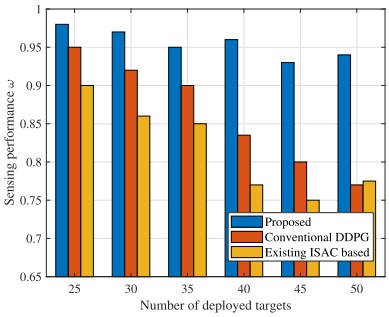

Fig. 12. Sensing performance vs. number of deployed targets.

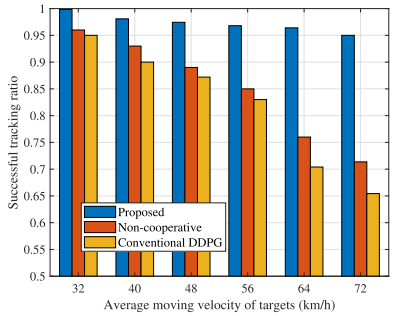

Fig. 13. Tracking ratio vs. moving velocity of targets.

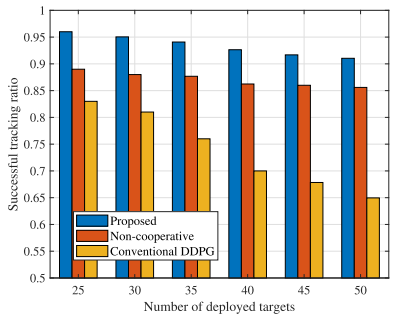

Fig. 14. Tracking ratio vs. number of deployed targets.

With the same parameters, Fig. 10f compares the latency overhead under different tracking velocities of UAVs. The latency is gradually reduced with the increase of the mobile speed of UAVs. Our algorithm realizes the low-latency performance compared to other benchmarks. The latency is acceptable when the average velocity of UAVs is 32 km/h while targets move at 56 km/h. In this case, our algorithm can rapidly discover the optimal neighbors to implement cooperative tracking. Meanwhile, our designed remote cooperation assists UAVs in transmitting data of targets to distant cooperators in real-time. Our algorithm efficiently reduces (66.7%, 77.9%) latency overhead compared to the DRL-based and Deep-Q learning-based algorithms.

Next, the sensing performance formulated in Eq. (5) is estimated under the scenario with 20 UAVs and 40 mobile targets. Fig. 11 shows the comparison of sensing performance as the iteration increases. On the whole, the sensing performance can promote as the iteration goes up. Since our algorithm can conduct UAVs to adjust their posture for valid sensing, high sensing performance is realized under a stable status. By contrast, the conventional DDPG algorithm can also ensure extensive sensing while incurring vast energy consumption in communication by frequent data exchange with a virtual center. Based on the joint consideration of sensing and communication, our algorithm promoting 14% sensing performance can achieve a comprehensive area coverage compared to the existing ISC-based algorithm.

In addition, the sensing performance is estimated under the given scenario with 30 UAVs and diverse targets in Fig. 12. In contrast to the benchmarks, the sensing performance can gradually improve as the number of targets increases. It implies that our lightweight cyber-twin system can conduct UAVs to perform dynamic sensing for time-varying targets. Explicitly, instead of collecting all the environmental information, our proposed lightweight cyber-twin system with a given attention mechanism only obtains the information of sensed targets and observed neighbors. It can significantly reduce imitation complexity and ensure real-time posture transfer for efficient target sensing. Our algorithm with the lightweight cyber-twin can improve the sensing performance by about 20% compared to the optimal DDPG algorithm in the dynamic UAV-MTT network.

The successful tracking ratio formulated by Eq. (6) is evaluated under the same scenario as in Fig. 11. Fig. 13 shows a comparison between the successful tracking ratio and the moving velocities of targets. We can find that our algorithm can always maintain the highest tracking ratio for different targets moving at diverse speeds. It implies that our designed lightweight mapping in the cyber-twin system can conduct remote UAVs to fly to feasible airspace locations for tracking highly moving targets. Compared to the non-cooperative tracking and conventional DDPG, our algorithm improves the successful tracking ratio by 21.0% and 26.3%, respectively.

Finally, the successful tracking ratio is verified under the different numbers of deployed targets in Fig. 14. The designed cyber-twin system can accurately track multiple targets in a given area. It can outperform the benchmarks by over 90% in terms of successful tracking ratio as the number of targets increases with 25 deployed UAVs with average 32 km/h speed. It is because our lightweight system can guide those remote UAVs for standby tracking. For the case of highly moving targets, our algorithm can promote a 7.6% and 29.3% success ratio compared with the non-cooperative tracking algorithm and the conventional DDPG algorithm.

Based on the results of Figs. 13 and 14, we can further analyze the relationship between the numbers of UAVs and

targets. With the 96% successful tracking ratio, 25 UAVs with an average 32 km/h speed can accurately track 25 targets with an average 56 km/h speed under the acceptable 1.5 s system response latency. Our system will provide a tracking service with more targets if we tolerate to reduce the successful tracking ratio. UAVs can sense mobile targets up to 50 with a 91.5% successful tracking ratio. In this case, we can dynamically adjust tracking indicators, including system response latency, successful tracking ratio, and flying velocity, to adapt to diverse tracking scenarios based on different requirements.

6.3 Performance Discussion

In the MTT system, the tracking performance is affected by the number of targets as well as the density of targets. The different number of targets and different densities can affect some system performance indicators such as tracking time and success ratio. In this work, we specifically analyze three important system performance indicators to estimate the impact of the number of targets and the target density on the tracking performance, including *system response time*, *system processing capability*, and *system error ratio*.

As a significant MTT performance indicator, the *system response time* can reflect the algorithm practicability. It includes sensing time, data processing latency, latency among UAVs, and decision-making time. It is noted that the training process is achieved based on an offline mode [45]. In Fig. 10d, we find that the response time of the designed algorithm is always less than 1.5 s as the number and density of mobile targets increase in the large-scale tracking area. The response time is stable when the number of targets is more than that of UAVs. In other words, our system can ensure the real-time tracking requirement with excess loads. It is lower than all the benchmarks.

The *system process capability* is given to analyze the algorithm effectiveness when the MTT system is overloaded (i.e., there exist numerous sensed targets with high density). The processing capability can be formulated as $\frac{1}{RT}$ [46], where RT denotes the system response time. In this context, we mainly focus on the software process capability with off-the-shelf onboard sensors and computers. Based on the simulation results, our system can cope with 500 mobile targets per second with a deployment density of 55.6 targets per km^2 under the given system latency requirement. Our system can improve the process capability of the existing ISAC-based algorithm by 81.25%.

With the stable system performance, the *system error ratio* can be estimated based on the timeout ratio. The timeout ratio reflects the tracking effectiveness that can be equivalent to the successful tracking ratio. In Fig. 14, the highly successful tracking performance with over 90% can be still obtained when the number of mobile targets is twice as many as that of UAVs. From Fig. 13, we can observe that 20 UAV with average 56 km/h speed can accurately track 40 targets with average 72 km/h speed. It ensure a 95% successful tracking ratio in the given $3\ km \times 3\ km$ area. Thereafter, our designed system is able to provide accurate and real-time tracking performance even in scenarios with a large number of tracking targets.

We also test the MTT system in practical scenarios shown in Fig. 8a. We deploy three UAVs and a single target. The trajectory of the target is collected based on the above-mentioned method. The sensing and tracking areas are the same circular region with a 30 m radius and constant flight height of 50 m. Trackers communicate with neighbors using WiFi devices in the Local Area Network (LAN). Trackers implement hover and rotation operations to detect the target and neighbors. Manifold computes the relative physical distance collected from sensors when target detection is successful. The imitation process is implemented in the Manifold. Trackers adjust postures based on the gyroscope sensor and move toward the target when the relative distance is over a given 25 m threshold.

In addition, the prediction information is transmitted to the neighbor based on socket communication technology. A socket is one endpoint of a two-way communication link between two programs running on the network. It is bound to a port number so that the Transmission Control Protocol (TCP) layer can identify the application to which data is destined to be sent. The neighbor also informs the remote tracker to move towards an assigned position that is smoothly implemented based on GPS. The energy consumption in communication with 6.2 J is computed based on the change in electric quantity. The system latency overhead is obtained by theoretical calculation with 1.3 s. Thereafter, the MTT can be extended into a large-scale scenario with multiple UAVs and targets. It is challenging to ensure safe flight and reliable data transmission. In this case, we can equip multiple laser-ranging sensors to acquire distance relations among UAVs and targets. The stable data transmission can be achieved by accessing moderate UAVs in the same LAN.

The ISC-based tracking cooperation is highly extendable based on data-driven and model-driven technologies for the UAV-MTT network. Inversely, traditional communications mainly focus on model-driven solutions, which directly depend on perfect datasets that are impossible to obtain, thus the energy consumption in communication is significantly increased for real-time MTT. This paper has provided enhanced communication and sensing for UAV cooperation and real-time MTT. Our algorithm is verified by multidimensional comparisons.

7 Conclusion

In this paper, we have designed a cooperative tracking framework to realize a high-efficient tracking for practical MTT scenarios. We propose a cyber-twin-based cooperative tracking algorithm. This algorithm achieves accurate tracking of heterogeneous targets with time-varying speeds. Explicitly, UAVs can use tailored cyber-twin models to coordinate suitable neighbors and remote UAVs for tracking cooperation, so that the communication overheads caused by the cooperation among UAVs can be significantly reduced. These contributions make our system outperform the benchmarks by up to 20.0% and 23.7%, in terms of system sensing performance and successful tracking ratio, respectively. However, the proposed framework introduces extra computing overheads due to this tailored cyber-twin model. The model maybe consume obvious computing

resource of UAVs to ensure accurate and real-time target estimation.

In the future, we will improve the flexibility of the tracking framework with the combination of centralized and distributed patterns, in which edge servers such as flying base stations are available [47]. The flexible framework may provide centralized management to assist distributed MTT in computing resource scheduling. In this context, the cybertwin model can be further optimized towards a more lightweight way while processing more comprehensive data through locally centralized management. Moreover, we will consider real-time information exchange operation with desired data as a part of future work as well.

REFERENCES

[1] T. Calamoneri and F. Corò, "A realistic model for rescue operations after an earthquake," in *Proc. 16th ACM Symp. QoS Secur. Wireless Mobile Netw.*, 2020, pp. 123–126.

[2] F. Liu, Y. Guo, Z. Cai, N. Xiao, and Z. Zhao, "Edge-enabled disaster rescue: A case study of searching for missing people," *ACM Trans. Intell. Syst. Technol.*, vol. 10, no. 6, Dec. 2019.

[3] X. Chen, S. Leng, J. He, and L. Zhou, "Deep-learning-based intelligent intervehicle distance control for 6G-enabled cooperative autonomous driving," *IEEE Internet Things J.*, vol. 8, no. 20, pp. 15 180–15 190, Oct. 2021.

[4] C. Luo, M. N. Satpute, D. Li, Y. Wang, W. Chen, and W. Wu, "Fine-grained trajectory optimization of multiple UAVs for efficient data gathering from WSNs," *IEEE/ACM Trans. Netw.*, vol. 29, no. 1, pp. 162–175, Feb. 2021.

[5] K. Xiong, S. Leng, J. Hu, X. Chen, and K. Yang, "Smart network slicing for vehicular fog-RANs," *IEEE Trans. Veh. Technol.*, vol. 68, no. 4, pp. 3075–3085, Apr. 2019.

[6] T. Feng, L. Xie, J. Yao, and J. Xu, "UAV-enabled data collection for wireless sensor networks with distributed beamforming," *IEEE Trans. Wireless Commun.* vol. 21, no. 2, pp. 1347–1361, Feb. 2022.

[7] G. Qiao, S. Leng, S. Maharjan, Y. Zhang, and N. Ansari, "Deep reinforcement learning for cooperative content caching in vehicular edge computing and networks," *IEEE Internet Things J.*, vol. 7, no. 1, pp. 247–257, Jan. 2020.

[8] F. Tao, H. Zhang, A. Liu, and A. Y. C. Nee, "Digital twin in industry: State-of-the-art," *IEEE Trans. Ind. Informat.*, vol. 15, no. 4, pp. 2405–2415, Apr. 2019.

[9] A. F. García-Fernández and W. Yi, "Continuous-discrete multiple target tracking with out-of-sequence measurements," *IEEE Trans. Signal Process.*, vol. 69, pp. 4699–4709, 2021.

[10] F. Meyer, P. Braca, P. Willett, and F. Hlawatsch, "A scalable algorithm for tracking an unknown number of targets using multiple sensors," *IEEE Trans. Signal Process.*, vol. 65, no. 13, pp. 3478–3493, Jul. 2017.

[11] O. E. Marai, T. Taleb, and J. Song, "Roads infrastructure digital twin: A step toward smarter cities realization," *IEEE Netw.*, vol. 35, no. 2, pp. 136–143, Mar./Apr. 2021.

[12] L. Lei, G. Shen, L. Zhang, and Z. Li, "Toward intelligent cooperation of UAV swarms: When machine learning meets digital twin," *IEEE Netw.*, vol. 35, no. 1, pp. 386–392, Jan./Feb. 2021.

[13] D. Guo, R. Y. Zhong, Y. Rong, and G. G. Q. Huang, "Synchronization of shop-floor logistics and manufacturing under IIoT and digital twin-enabled graduation intelligent manufacturing system," *IEEE Trans. Cybern.*, early access, Sep. 13, 2021, doi: 10.1109/TCYB.2021.3108546.

[14] B. J. Southwell, J. W. Cheong, and A. G. Dempster, "A matched filter for spaceborne GNSS-R based sea-target detection," *IEEE Trans. Geosci. Remote Sens.*, vol. 58, no. 8, pp. 5922–5931, Aug. 2020.

[15] H. Kang, Q. Zhang, and Q. Huang, "Context-aware wireless-based cross-domain gesture recognition," *IEEE Internet Things J.*, vol. 8, no. 17, pp. 13 503–13 515, Sep. 2021.

[16] F. Y. P. Feng, M. Rihan, and L. Huang, "Positional perturbations analysis for micro-UAV array with relative position-based formation," *IEEE Commun. Lett.*, vol. 25, no. 9, pp. 2918–2922, Sep. 2021.

[17] Q. Huang, G. Song, W. Wang, H. Dong, J. Zhang, and Q. Zhang, "FreeScatter: Enabling concurrent backscatter communication using antenna arrays," *IEEE Internet Things J.*, vol. 7, no. 8, pp. 7310–7318, Aug. 2020.

[18] M. Mozaffari, W. Saad, M. Bennis, Y.-H. Nam, and M. Debbah, "A tutorial on UAVs for wireless networks: Applications, challenges, and open problems," *IEEE Commun. Surv. Tut.*, vol. 21, no. 3, pp. 2334–2360, Jul.–Sep. 2019.

[19] S. Chai and V. K. N. Lau, "Multi-UAV trajectory and power optimization for cached UAV wireless networks with energy and content recharging-demand driven deep learning approach," *IEEE J. Sel. Areas Commun.*, vol. 39, no. 10, pp. 3208–3224, Oct. 2021.

[20] H. Yu, K. Meier, M. Argyle, and R. W. Beard, "Cooperative path planning for target tracking in urban environments using unmanned air and ground vehicles," *IEEE/ASME Trans. Mechatronics*, vol. 20, no. 2, pp. 541–552, Apr. 2015.

[21] Y. Liu, Q. Wang, H. Hu, and Y. He, "A novel real-time moving target tracking and path planning system for a quadrotor UAV in unknown unstructured outdoor scenes," *IEEE Trans. Syst., Man, Cybern. Syst.*, vol. 49, no. 11, pp. 2362–2372, Nov. 2019.

[22] T. Oliveira, A. P. Aguiar, and P. Encarnação, "Moving path following for unmanned aerial vehicles with applications to single and multiple target tracking problems," *IEEE Trans. Robot.*, vol. 32, no. 5, pp. 1062–1078, Oct. 2016.

[23] M. Khan, K. Heurtefeux, A. Mohamed, K. A. Harras, and M. M. Hassan, "Mobile target coverage and tracking on drone-be-gone UAV cyber-physical testbed," *IEEE Syst. J.*, vol. 12, no. 4, pp. 3485–3496, Dec. 2018.

[24] H. Guo, C. Shen, H. Zhang, H. Chen, and R. Jia, "Simultaneous trajectory planning and tracking using an MPC method for cyber-physical systems: A case study of obstacle avoidance for an intelligent vehicle," *IEEE Trans. Ind. Informat.*, vol. 14, no. 9, pp. 4273–4283, Sep. 2018.

[25] B. Wang, B. Zhang, and R. Su, "Optimal tracking cooperative control for cyber-physical systems: Dynamic fault-tolerant control and resilient management," *IEEE Trans. Ind. Informat.*, vol. 17, no. 1, pp. 158–167, Jan. 2021.

[26] M. Y. Arafat and S. Moh, "Localization and clustering based on swarm intelligence in uav networks for emergency communications," *IEEE Internet Things J.*, vol. 6, no. 5, pp. 8958–8976, Oct. 2019.

[27] S. Kim, D. Kwon, and Y. Ji, "CNN based human detection for unmanned aerial vehicle (poster)," in *Proc. 17th Annu. Int. Conf. Mobile Syst., Appl., Serv.*, 2019, pp. 626–627.

[28] M. Trobinger, D. Vecchia, D. Lobba, T. Istomin, and G. P. Picco, "One flood to route them all: Ultra-fast convergecast of concurrent flows over UWB," in *Proc. 18th ACM Conf. Embedded Netw. Sensor Syst.*, 2020, pp. 179–191.

[29] A. Trotta, M. D. Felice, F. Montori, K. R. Chowdhury, and L. Bononi, "Joint coverage, connectivity, and charging strategies for distributed UAV networks," *IEEE Trans. Robot.*, vol. 34, no. 4, pp. 883–900, Aug. 2018.

[30] L. Lamport, "Time, clocks, and the ordering of events in a distributed system," *Commun. ACM*, vol. 21, no. 7, pp. 558–565, Jul. 1978.

[31] W. Feng *et al.*, "Hybrid beamforming design and resource allocation for UAV-aided wireless-powered mobile edge computing networks with NOMA," *IEEE J. Sel. Areas Commun.*, vol. 39, no. 11, pp. 3271–3286, Nov. 2021.

[32] J. G. Andrews, T. Bai, M. N. Kulkarni, A. Alkhateeb, A. K. Gupta, and R. W. Heath, "Modeling and analyzing millimeter wave cellular systems," *IEEE Trans. Commun.*, vol. 65, no. 1, pp. 403–430, Jan. 2017.

[33] X. Gu, H. Soury, and B. Smida, "On the throughput of wireless communication with combined CSI and H-ARQ feedback," *IEEE Open J. Commun. Soc.*, vol. 2, pp. 439–455, 2021.

[34] L. P. Perera, P. Oliveira, and C. Guedes Soares, "Maritime traffic monitoring based on vessel detection, tracking, state estimation, and trajectory prediction," *IEEE Trans. Intell. Transp. Syst.*, vol. 13, no. 3, pp. 1188–1200, Sep. 2012.

[35] P. Frogerais, J.-J. Bellanger, and L. Senhadji, "Various ways to compute the continuous-discrete extended kalman filter," *IEEE Trans. Autom. Control*, vol. 57, no. 4, pp. 1000–1004, Apr. 2012.

[36] Y. Zeng, J. Xu, and R. Zhang, "Energy minimization for wireless communication with rotary-wing UAV," *IEEE Trans. Wireless Commun.*, vol. 18, no. 4, pp. 2329–2345, Apr. 2019.

[37] X. Zhang, Y. Yang, Z. Li, X. Ning, Y. Qin, and W. Cai, "An improved encoder-decoder network based on strip pool method applied to segmentation of farmland vacancy field," *Entropy*, vol. 23, no. 4, 2021, Art. no. 435.
[38] Z. Qin, H. Yao, and T. Mai, "Traffic optimization in satellites communications: A multi-agent reinforcement learning approach," in *Proc. Int. Wireless Commun. Mobile Comput.*, 2020, pp. 269–273.
[39] T. J. Ypma, "Historical development of the newton–raphson method," *SIAM Rev.*, vol. 37, no. 4, pp. 531–551, 1995.
[40] K. Cai, H. Chen, W. Ai, X. Miao, Q. Lin, and Q. Feng, "Feedback convolutional network for intelligent data fusion based on near-infrared collaborative IoT technology," *IEEE Trans. Ind. Informat.*, vol. 18, no. 2, pp. 1200–1209, Feb. 2022.
[41] H. Mao, Z. Zhang, Z. Xiao, Z. Gong, and Y. Ni, "Learning multi-agent communication with double attentional deep reinforcement learning," *Auton. Agents Multi-Agent Syst.*, vol. 34, no. 1, 2020, Art. no. 32.
[42] X. Chen, Z. Feng, Z. Wei, F. Gao, and X. Yuan, "Performance of joint sensing-communication cooperative sensing uav network," *IEEE Trans. Veh. Technol.*, vol. 69, no. 12, pp. 15 545–15 556, 2020.
[43] W. Chen *et al.*, "Maddpg algorithm for coordinated welding of multiple robots," in *Proc. 6th Int. Conf. Automat., Control Robot. Eng.*, 2021, pp. 1–5.
[44] J. N. Foerster, Y. M. Assael, N. De Freitas, and S. Whiteson, "Learning to communicate with deep multi-agent reinforcement learning," 2016, *arXiv:1605.06676*.
[45] R. Agarwal, D. Schuurmans, and M. Norouzi, "An optimistic perspective on offline reinforcement learning," in *Proc. Int. Conf. Mach. Lear.*, 2020, pp. 104–114.
[46] R. L. Nolan, "Managing the computer resource: A stage hypothesis," *Commun. ACM*, vol. 16, no. 7, pp. 399–405, Jul. 1973.
[47] M. Nikooroo and Z. Becvar, "Optimization of total power consumed by flying base station serving mobile users," *IEEE Trans. Netw. Sci. Eng.*, vol. 9, no. 4, pp. 2815–2832, Jul./Aug. 2022.

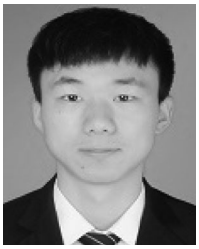

Longyu Zhou (Graduate Student Member, IEEE) is currently working toward the PhD degree with the School of Information and Communication Engineering, University of Electronic Science and Technology of China (UESTC). He is also working with the Embedded and Networking System (ENS) group, Delft University of Technology as a visiting student. His research interests include Internet of Things, edge intelligence, resource scheduling, and wireless sensor networks. He was a recipient of the Best Paper Award in 20th IEEE Conference on Communications and Technology. He also serves/has serves as a reviewer and a TPC member for the IEEE Global Communications Conference (Globecom), the IEEE International Conference on Communications (ICC), etc.

Supeng Leng (Member, IEEE) received the PhD degree from Nanyang Technological University (NTU), Singapore. He is currently a full professor and the vice dean with the School of Information and Communication Engineering, University of Electronic Science and Technology of China. He is also the leader of the research group of Ubiquitous Wireless Networks. He is a research fellow with the Network Technology Research Center, NTU. He has authored or coauthored more than 180 research papers and four books/book chapters in recent years. His research interests include resource, spectrum, energy, routing and networking in Internet of Things, vehicular networks, broadband wireless access networks, and the next generation intelligent mobile networks. He was the recipient of the Best Paper Awards at four IEEE international conferences. He is an organizing committee chair and the TPC member for many international conferences, and a reviewer of more than 20 well-known academic international journals.

Qing Wang (Senior Member, IEEE) received the PhD degree from UC3M and IMDEA Networks Institute, Spain, in 2016. He is currently an assistant professor with the Embedded and Networked Systems Group of the Delft University of Technology, the Netherlands. His research interests include visible light communication and sensing systems, and the Internet of Things. He is the co-founder of OpenVLC, an open-source and low-cost platform for VLC research. His research outcomes on active/passive visible light communication and sensing systems have been published at IEEE/ACM conferences and journals such as ACM MobiCom, CoNEXT, SenSys, IEEE INFOCOM, *IEEE/ACM Transactions on Networking*, and *IEEE Journal on Selected Areas in Communications*. He has received several awards, including the MobiCom Honourable Mention Award (2020), COMSNETS Best Paper Award (2019), Accenture Innovation Award (2017), Best Paper Runner Up with CoNEXT (2016), etc.

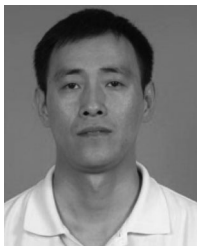

Qiang Liu (Member, IEEE) received the BS, MS and PhD degrees from the University of Electronic Science and Technology of China (UESTC), in 1996, 2000, and 2012, respectively. After graduating from MS study, in 2000, he has worked with School of Communication and Information Engineering, UESTC, China, and is an associate professor now. He had worked in the University of Essex in U.K. (2012–2013) and the University of California, Davis in U.S.A (2017–2018) as a visitor scholar. His researches interests include wireless sensor networks, Internet of Things, broadband wireless networks and molecular communication. He is the member of IEEE/IEEE ComSoc. He is the reviewer of *IEEE Transactions on Nano-Bioscience*, *International Journal of Communication Systems (IJCS)*.